

---

---

**Universiteit Utrecht**



*Department  
of Mathematics*

**Efficient computation of multivariable  
transfer function dominant poles using  
subspace acceleration**

by

**Joost Rommes and Nelson Martins**

---

Preprint

nr. 1344

January, 2006

---

# Efficient computation of multivariable transfer function dominant poles using subspace acceleration

Joost Rommes\* and Nelson Martins†

January, 2006

## Abstract

This paper describes a new algorithm to compute the dominant poles of a high-order multi-input multi-output (MIMO) transfer function. The algorithm, called the Subspace Accelerated MIMO Dominant Pole Algorithm (SAMDP), is able to compute the full set of dominant poles efficiently. SAMDP can be used to produce good modal equivalents automatically. The general algorithm is robust, applicable to both square and non-square transfer function matrices, and can easily be tuned to suit different practical system needs.

## 1 Introduction

Current model reduction techniques for power system stability analysis and controller design [1–5] produce good results but are not applicable to large scale problems. If only a small part of the system pole spectrum is controllable-observable for the transfer function, a low-cost alternative for large-scale systems is modal model reduction. Modal reduction approximates the transfer function by a modal equivalent that is computed from the dominant poles and their corresponding residues. To produce a good modal equivalent, specialized eigensolution methods are needed. An algorithm that automatically and efficiently computes the full set of dominant poles of a scalar transfer function was presented recently [6], but existing methods for multi-input multi-output (MIMO) transfer functions [7] are not capable enough to produce good modal equivalents automatically. A survey on model reduction methods employing either singular value decompositions or moment matching based methods is found in [8, 9]. An introduction on modal model reduction on state space models can be found in [10], while [11] describes a possible enhancement to modal model reduction.

In this article, a new extension of the Subspace Accelerated Dominant Pole Algorithm (SADPA) [6] will be proposed: Subspace Accelerated MIMO Dominant Pole Algorithm (SAMDP). The SADPA is a generalization of the Dominant Pole Algorithm [12], that automatically computes a high quality modal equivalent of a transfer function. The SAMDP can also be seen as a generalization of the MIMO Dominant Pole algorithm [7]. SAMDP computes the dominant poles and corresponding residue matrices one by one by selecting the most dominant approximation every iteration. This approach leads to a faster, more robust and more flexible algorithm. To avoid repeated computation of the same dominant poles, a deflation strategy is used. The SAMDP directly operates on implicit state space systems, also known as descriptor systems, which are very sparse in practical power system applications.

The article is organized as follows. Section 2 summarizes some well known properties of MIMO transfer functions and formulates the problem of computing the dominant poles of a MIMO transfer function. Section 3 describes the new SAMDP algorithm. In section 4, numerical aspects concerning practical implementations of SAMDP are discussed. Extensive numerical results are presented in 5. Section 6 concludes.

---

\*Joost Rommes is with Mathematical Institute, Utrecht University, P.O.Box 80100, 3508 TA Utrecht, The Netherlands (rommes@math.uu.nl).

†Nelson Martins is with CEPEL, P.O.Box 68007 - Rio de Janeiro, RJ - 20001 - 970, Brazil (nelson@cepel.br).

## 2 MIMO transfer functions, sigma plots and dominant poles

For a multi-input multi-output (MIMO) system

$$\begin{cases} \dot{\mathbf{x}}(t) &= A\mathbf{x}(t) + B\mathbf{u}(t) \\ \mathbf{y}(t) &= C^T\mathbf{x}(t) + D\mathbf{u}(t), \end{cases} \quad (1)$$

where  $A \in \mathbb{R}^{n \times n}$ ,  $B \in \mathbb{R}^{n \times m}$ ,  $C \in \mathbb{R}^{p \times n}$ ,  $\mathbf{x}(t) \in \mathbb{R}^n$ ,  $\mathbf{u}(t) \in \mathbb{R}^m$ ,  $\mathbf{y}(t) \in \mathbb{R}^p$  and  $D \in \mathbb{R}^{p \times m}$ , the transfer function  $H(s) : \mathbb{C} \rightarrow \mathbb{C}^{p \times m}$  is defined as

$$H(s) = C^T(sI - A)^{-1}B + D, \quad (2)$$

where  $I \in \mathbb{R}^{n \times n}$  is the identity matrix and  $s \in \mathbb{C}$ . Without loss of generality,  $D = 0$  in the following.

It is well known that the transfer function of single-input single-output system is defined by a complex number for any frequency. For a MIMO system, the transfer function is a  $p \times m$  matrix and hence does not have a unique gain for a given frequency. The SISO concept of a single transfer function gain must be replaced by a range of gains that have an upper bound for non-square matrices  $H(s)$ , and both upper and lower bounds for square matrices  $H(s)$ . Denoting the smallest and largest singular values [13] of  $H(j\omega)$  by  $\sigma_{\min}(\omega)$  and  $\sigma_{\max}(\omega)$ , it follows for square  $H(s)$  that

$$\sigma_{\min}(j\omega) \leq \frac{\|H(j\omega)\mathbf{u}(j\omega)\|_2}{\|\mathbf{u}(j\omega)\|_2} \leq \sigma_{\max}(j\omega),$$

ie. for a given frequency  $\omega$ , the gain of a MIMO transfer function is between the smallest and largest singular value of  $H(j\omega)$ , which are also called the smallest and largest principal gains [14]. For non-square transfer functions  $H(s)$ , only the upper bound holds. Plots of the smallest and largest principal gains against frequency, also known as sigma plots, are used in the robust control design and analysis of MIMO systems [14].

Let the eigenvalues (poles) of  $A$  and the corresponding right and left eigenvectors be given by the triplets  $(\lambda_j, \mathbf{x}_j, \mathbf{y}_j)$ , and let the right and left eigenvectors be scaled so that  $\mathbf{y}_j^* \mathbf{x}_j = 1$ . Note that  $\mathbf{y}_j^* \mathbf{x}_k = 0$  for  $j \neq k$ . The transfer function  $H(s)$  can be expressed as a sum of residue matrices  $R_j \in \mathbb{C}^{p \times m}$  over first order poles [15]:

$$H(s) = \sum_{j=1}^n \frac{R_j}{s - \lambda_j},$$

where the residue matrices  $R_j$  are

$$R_j = (C^T \mathbf{x}_j)(\mathbf{y}_j^* B).$$

A pole  $\lambda_j$  that corresponds to a residue  $R_j$  with large norm  $\|R_j\|_2 = \sigma_{\max}(R_j)$  is called a dominant pole, i.e. a pole that is well observable and controllable in the transfer function. This can also be observed from the corresponding  $\sigma_{\max}$ -plot of  $H(s)$ , where peaks occur at frequencies close to the imaginary parts of the dominant poles of  $H(s)$ . An approximation of  $H(s)$  that consists of  $k < n$  terms with  $\|R_j\|_2$  above some value, determines the effective transfer function behaviour [16] and will be referred to as transfer function modal equivalent:

$$H_k(s) = \sum_{j=1}^k \frac{R_j}{s - \lambda_j},$$

Because a residue matrix  $R_j$  is the product of a column vector and a row vector, it is of unit rank. Therefore at least  $\min(m, p)$  different poles are needed to obtain a modal equivalent with nonzero  $\sigma_{\min}(\omega)$  plot [7, 17].

The problem of concern can now be formulated as: Given a MIMO linear, time invariant, dynamical system  $(A, B, C, D)$ , compute  $k \ll n$  dominant poles  $\lambda_j$  and the corresponding right and left eigenvectors  $\mathbf{x}_j$  and  $\mathbf{y}_j$ .

### 3 Subspace Accelerated MIMO Dominant Pole Algorithm (SAMDP)

The subspace accelerated MIMO dominant pole algorithm (SAMDP) is based on the dominant pole algorithm (DPA) [12], the subspace accelerated DPA (SADPA) [6] and the MIMO dominant pole algorithm (MDP) [7]. First, a Newton scheme will be derived for computing the dominant poles of a MIMO transfer function. Then, the SAMDP will be formulated as an accelerated Newton scheme, using the same improvements that were used in the robust SADPA algorithm.

All algorithms are described as directly operating on the state-space model. The practical implementations (see section 4.1) operate on the sparse descriptor system model, which is the unreduced Jacobian for the power system stability problem, analyzed in the examples of this paper (see section 5).

#### 3.1 Newton scheme for computing dominant poles

The dominant poles of a MIMO transfer function  $H(s) = C^T(sI - A)^{-1}B$  are those  $s \in \mathbb{C}$  for which  $\sigma_{\max}(H(s)) \rightarrow \infty$ . For square transfer functions ( $m = p$ ), there is an equivalent criterion: the dominant poles are those  $s \in \mathbb{C}$  for which  $\lambda_{\min}(H^{-1}(s)) \rightarrow 0$ . In the following it will be assumed that  $m = p$ ; for general MIMO transfer functions, see 4.3.

The Newton method can be used to find the  $s \in \mathbb{C}$  for which the objective function

$$f : \mathbb{C} \longrightarrow \mathbb{C} : s \longmapsto \lambda_{\min}((C^T(sI - A)^{-1}B)^{-1}) \quad (3)$$

is zero. Let  $(\mu(s), \mathbf{u}(s), \mathbf{v}(s))$  be an eigentriplet of  $H^{-1}(s) \in \mathbb{C}^{m \times m}$ , ie.  $H^{-1}(s)\mathbf{u}(s) = \mu(s)\mathbf{u}(s)$  and  $\mathbf{v}^*(s)H^{-1}(s) = \mu(s)\mathbf{v}^*(s)$ , with  $\mathbf{v}^*(s)\mathbf{u}(s) = 1$ . The derivative of  $\mu(s)$  is given by [18]

$$\frac{d\mu}{ds}(s) = \mathbf{v}^*(s) \frac{dH^{-1}}{ds}(s) \mathbf{u}(s), \quad (4)$$

where

$$\begin{aligned} \frac{dH^{-1}}{ds}(s) &= -H^{-1}(s) \frac{dH}{ds}(s) H^{-1}(s) \\ &= H^{-1}(s) C^T (sI - A)^{-2} B H^{-1}(s). \end{aligned} \quad (5)$$

Note that it is assumed that  $H^{-1}(s)$  has distinct eigenvalues and that the function that selects  $\mu_{\min}(s)$  has derivative 1. Substituting (5) in (4), it follows that

$$\begin{aligned} \frac{d\mu}{ds}(s) &= \mathbf{v}^*(s) H^{-1}(s) C^T (sI - A)^{-2} B H^{-1}(s) \mathbf{u}(s) \\ &= \mu^2(s) \mathbf{v}^*(s) C^T (sI - A)^{-2} B \mathbf{u}(s). \end{aligned}$$

The Newton scheme then becomes

$$\begin{aligned} s^{k+1} &= s^k - \frac{f(s^k)}{f'(s^k)} \\ &= s^k - \frac{\mu_{\min}}{\mu_{\min}^2 \mathbf{v}^* C^T (s^k I - A)^{-2} B \mathbf{u}} \\ &= s^k - \frac{1}{\mu_{\min} \mathbf{v}^* C^T (s^k I - A)^{-2} B \mathbf{u}}, \end{aligned}$$

where  $(\mu_{\min}, \mathbf{u}, \mathbf{v}) = (\mu_{\min}(s^k), \mathbf{u}_{\min}(s^k), \mathbf{v}_{\min}^*(s^k))$  is the eigentriplet of  $H^{-1}(s^k)$  corresponding to  $\lambda_{\min}(H^{-1}(s^k))$ . An algorithm, very similar to the DPA algorithm [12], for the computation of single dominant pole of a MIMO transfer function using the above Newton scheme, is shown in Alg. 1. In the neighborhood of a solution, Alg. 1 converges quadratically.

---

**Algorithm 1** A MIMO Dominant Pole Algorithm.

---

**INPUT:** System  $(A, B, C)$ , initial pole estimate  $s_1$

**OUTPUT:** Dominant pole  $\lambda$  and corresponding right and left eigenvectors  $\mathbf{x}$  and  $\mathbf{y}$ .

1: Set  $k = 1$

2: **while** not converged **do**

3:   Compute eigentriplet  $(\mu_{\min}, \mathbf{u}, \mathbf{v})$  of  $H^{-1}(s_k)$

4:   Solve  $\mathbf{x} \in \mathbb{C}^n$  from

$$(s_k I - A)\mathbf{x} = B\mathbf{u}$$

5:   Solve  $\mathbf{y} \in \mathbb{C}^n$  from

$$(s_k I - A)^*\mathbf{y} = C\mathbf{v}$$

6:   Compute the new pole estimate

$$s_{k+1} = s_k - \frac{1}{\mu_{\min}} \frac{1}{\mathbf{y}^* \mathbf{x}}$$

7:   The pole  $\lambda = s_{k+1}$  has converged if

$$\|A\mathbf{x} - s_{k+1}\mathbf{x}\|_2 < \epsilon$$

    for some  $\epsilon \ll 1$

8:   Set  $k = k + 1$

9: **end while**

---

## 3.2 SAMDP as an accelerated Newton scheme

The three strategies that are used for SADPA [6], are also used to make SAMDP, a generalization of Alg. 1: subspace acceleration, selection of most dominant approximation and deflation. A global overview of the SAMDP is shown in Alg. 2. Each of the three strategies is explained in the following paragraphs.

### 3.2.1 Subspace acceleration

The approximations  $\mathbf{x}$  and  $\mathbf{y}$  that are computed in steps 4 and 5 of Alg. 1 are kept in orthogonal search spaces  $X$  and  $Y$ , using modified Gram-Schmidt (MGS) [13]. These search spaces grow every iteration and will contain better approximations (see step 6 and 7 of Alg. 2).

### 3.2.2 Selection strategy

Every iteration a new pole estimate  $s_k$  must be chosen. There are several strategies (see [6] and section 4.2). Here the most natural choice is to select the triplet  $(\hat{\lambda}_j, \hat{\mathbf{x}}_j, \hat{\mathbf{y}}_j)$  with largest residue norm  $\|\hat{R}_j\|_2$ . SAMDP continues with  $s_{k+1} = \hat{\lambda}_j$ . See Alg. 3.

---

**Algorithm 3**  $(\Lambda, X, Y) = \text{Sort}(\Lambda, X, Y, B, C)$

---

**INPUT:**  $\Lambda \in \mathbb{C}^n$ ,  $X, Y \in \mathbb{C}^{n \times k}$ ,  $B \in \mathbb{R}^{n \times p}$ ,  $C \in \mathbb{R}^{n \times m}$

**OUTPUT:**  $\Lambda \in \mathbb{C}^n$ ,  $X, Y \in \mathbb{C}^{n \times k}$  with  $\lambda_1$  the pole with largest residue matrix norm and  $\mathbf{x}_1$  and  $\mathbf{y}_1$  the corresponding approximate right and left eigenvectors.

1: Compute residue matrices  $R_i = (C^T \mathbf{x}_i)(\mathbf{y}_i^* B)$

2: Sort  $\Lambda$ ,  $X$ ,  $Y$  in decreasing  $\|R_i\|_2$  order

---

### 3.2.3 Deflation

An eigentriplet  $(\hat{\lambda}_j, \hat{\mathbf{x}}_j, \hat{\mathbf{y}}_j)$  has converged if  $\|A\hat{\mathbf{x}}_j - \hat{\lambda}_j\hat{\mathbf{x}}_j\|_2$  is smaller than some tolerance  $\epsilon$ . If more than one eigentriplet is wanted, repeated computation of already converged eigentriplets

---

**Algorithm 2** Subspace Accelerated MDP Algorithm.

---

**INPUT:** System  $(A, B, C)$ , initial pole estimate  $s_1$  and the number of wanted poles  $p_{max}$

**OUTPUT:** Dominant pole triplets  $(\lambda_i, \mathbf{r}_i, \mathbf{l}_i)$ ,  $i = 1, \dots, p_{max}$

1:  $k = 1$ ,  $p_{found} = 0$ ,  $X = Y = \Lambda = R = L = []$

2: **while**  $p_{found} < p_{max}$  **do**

3:   Compute eigentriplet  $(\mu_{\min}, \mathbf{u}, \mathbf{v})$  of  $H^{-1}(s_k)$

4:   Solve  $\mathbf{x} \in \mathbb{C}^n$  from

$$(s_k I - A)\mathbf{x} = B\mathbf{u}$$

5:   Solve  $\mathbf{y} \in \mathbb{C}^n$  from

$$(s_k I - A)^*\mathbf{y} = C\mathbf{v}$$

6:    $X = \text{Expand}(X, R, L, \mathbf{x})$  {Alg. 4}

7:    $Y = \text{Expand}(Y, L, R, \mathbf{y})$  {Alg. 4}

8:   Compute  $G = Y^*X$  and  $T = Y^*AX$

9:   Compute eigentriplets of  $(T, G)$ :

$$(\tilde{\lambda}_i, \tilde{\mathbf{x}}_i, \tilde{\mathbf{y}}_i), \quad i = 1, \dots, k$$

10:   Compute approximate eigentriplets of  $A$  as

$$(\hat{\lambda}_i = \tilde{\lambda}_i, \hat{\mathbf{x}}_i = X\tilde{\mathbf{x}}_i, \hat{\mathbf{y}}_i = Y\tilde{\mathbf{y}}_i), \quad i = 1, \dots, k$$

11:    $\hat{\Lambda} = [\hat{\lambda}_1, \dots, \hat{\lambda}_k]$

12:    $\hat{X} = [\hat{\mathbf{x}}_1, \dots, \hat{\mathbf{x}}_k]$

13:    $\hat{Y} = [\hat{\mathbf{y}}_1, \dots, \hat{\mathbf{y}}_k]$

14:    $(\hat{\Lambda}, \hat{X}, \hat{Y}) = \text{Sort}(\hat{\Lambda}, \hat{X}, \hat{Y}, B, C)$  {Alg. 3}

15:   **if**  $\|A\hat{\mathbf{x}}_1 - \hat{\lambda}_1\hat{\mathbf{x}}_1\|_2 < \epsilon$  **then**

16:      $(\Lambda, R, L, X, Y) =$

$\text{Deflate}(\hat{\lambda}_1, \hat{\mathbf{x}}_1, \hat{\mathbf{y}}_1, \Lambda, R, L, \hat{X}_{2:k}, \hat{Y}_{2:k})$  {Alg. 5}

17:      $p_{found} = p_{found} + 1$

18:     Set  $\hat{\lambda}_1 = \hat{\lambda}_2$

19:   **end if**

20:   Set  $k = k + 1$

21:   Set the new pole estimate  $s_{k+1} = \hat{\lambda}_1$

22: **end while**

---

must be avoided. This can be achieved by using deflation [19,20].

If already the right and left eigenvectors  $\mathbf{x}_j$  and  $\mathbf{y}_j$  are found, then it can be verified that, if the exact vectors are found, the matrix

$$\tilde{A} = \Pi_j(I - \frac{\mathbf{x}_j \mathbf{y}_j^*}{\mathbf{y}_j^* \mathbf{x}_j}) \cdot A \cdot \Pi_j(I - \frac{\mathbf{x}_j \mathbf{y}_j^*}{\mathbf{y}_j^* \mathbf{x}_j})$$

has the same eigentriplets as  $A$ , but with the found eigenvalues transformed to zero.

Using this, the space  $X$  needs to be orthogonally expanded with  $\Pi_j(I - \frac{\mathbf{x}_j \mathbf{y}_j^*}{\mathbf{y}_j^* \mathbf{x}_j}) \cdot \mathbf{x}$  and similarly, the space  $Y$  needs to be orthogonally expanded with  $\Pi_j(I - \frac{\mathbf{y}_j \mathbf{x}_j^*}{\mathbf{x}_j^* \mathbf{y}_j}) \cdot \mathbf{y}$ . These projections are implemented using modified Gram-Schmidt (MGS) (see Alg. 4).

---

**Algorithm 4**  $X = \text{Expand}(X, R, L, \mathbf{x})$

---

**INPUT:**  $X \in \mathbb{C}^{n \times k}$  with  $X^* X = I$ ,  $R, L \in \mathbb{C}^{n \times p}$ ,  $\mathbf{x} \in \mathbb{C}^n$

**OUTPUT:**  $X \in \mathbb{C}^{n \times (k+1)}$  with  $X^* X = I$  and

$$\mathbf{x}_{k+1} = \Pi_{j=1}^p (I - \frac{\mathbf{r}_j \mathbf{l}_j^*}{\mathbf{l}_j^* \mathbf{r}_j}) \cdot \mathbf{x}$$

1:  $\mathbf{x} = \Pi_{j=1}^p (I - \frac{\mathbf{r}_j \mathbf{l}_j^*}{\mathbf{l}_j^* \mathbf{r}_j}) \cdot \mathbf{x}$

2:  $\mathbf{x} = \text{MGS}(X, \mathbf{x})$

3:  $X = [X, \mathbf{x} / \|\mathbf{x}\|_2]$

---

If a complex pole has converged, its complex conjugate is also a pole and the corresponding complex conjugate right and left eigenvectors can also be deflated. A complex conjugated pair is counted as one pole. The complete deflation procedure is shown in algorithm 5.

---

**Algorithm 5**

$(\Lambda, R, L, \tilde{X}, \tilde{Y}) = \text{Deflate}(\lambda, \mathbf{x}, \mathbf{y}, \Lambda, R, L, X, Y)$

---

**INPUT:**  $\lambda \in \mathbb{C}$ ,  $\mathbf{x}, \mathbf{y} \in \mathbb{C}^n$ ,  $\Lambda \in \mathbb{C}^p$ ,  $R, L \in \mathbb{C}^{n \times p}$ ,

$$X, Y \in \mathbb{C}^{n \times k}$$

**OUTPUT:**  $\Lambda \in \mathbb{C}^q$ ,  $R, L \in \mathbb{C}^{n \times q}$ ,  $\tilde{X}, \tilde{Y} \in \mathbb{C}^{n \times (k-q)}$ , where  $q = 1$  if  $\lambda$  has zero imaginary part and  $q = 2$  if  $\lambda$  has nonzero imaginary part.

1:  $\Lambda = [\Lambda, \lambda]$

2:  $R = [R, \mathbf{x}]$

3:  $L = [L, \mathbf{y}]$

4:  $q = 1$

5: **if**  $\text{imag}(\lambda) \neq 0$  **then**

6:   {Also deflate complex conjugate}

7:    $\Lambda = [\Lambda, \bar{\lambda}]$

8:    $R = [R, \bar{\mathbf{x}}]$

9:    $L = [L, \bar{\mathbf{y}}]$

10:    $q = 2$

11: **end if**

12:  $\tilde{X} = \tilde{Y} = []$

13: **for**  $j = 1, \dots, k - 1$  **do**

14:    $\tilde{X} = \text{Expand}(\tilde{X}, R, L, X_j)$

15:    $\tilde{Y} = \text{Expand}(\tilde{Y}, L, R, Y_j)$

16: **end for**

---

## 4 Practical implementations of SAMDP

In this section, aspects concerning practical implementations of SAMDP and the generalization of SAMDP to non-square MIMO transfer functions ( $m \neq p$ ) are discussed.

## 4.1 Sparse descriptor system models

The sparse descriptor system formulation of (1) becomes

$$\begin{cases} I_d \dot{\mathbf{x}}(t) &= A\mathbf{x}(t) + Bu(t) \\ y(t) &= C^T \mathbf{x}(t) + Du(t), \end{cases} \quad (6)$$

where  $A \in \mathbb{R}^{N \times N}$ ,  $B \in \mathbb{R}^{N \times m}$ ,  $C \in \mathbb{R}^{N \times p}$ ,  $\mathbf{x}(t) \in \mathbb{R}^N$ ,  $u(t) \in \mathbb{R}^m$ ,  $y(t) \in \mathbb{R}^p$ ,  $D \in \mathbb{R}^{p \times m}$  and  $I_d \in \mathbb{R}^{N \times N}$  is a diagonal matrix with diagonal elements either 0 or 1. The corresponding transfer function  $H_d(s) : \mathbb{C} \rightarrow \mathbb{C}^{p \times m}$  is defined as

$$H_d(s) = C^T (sI_d - A)^{-1} B + D, \quad (7)$$

where  $s \in \mathbb{C}$ . Without loss of generality,  $D = 0$  in the following.

The algorithms presented in this paper can easily be adapted to handle sparse descriptor systems. The changes essentially boil down to replacing  $I$  by  $I_d$  on most places and noting that for eigentriplets  $(\lambda_j, \mathbf{x}_j, \mathbf{y}_j)$  the relation  $\mathbf{y}_i^* I_d \mathbf{x}_j = 0, i \neq j$  holds. For completeness, the changes are given for each algorithm:

- Algorithm 1:

- Replace  $I$  by  $I_d$  in step 4 and 5.
- Step 6 becomes

$$s_{k+1} = s_k - \frac{1}{\mu_{\min}} \frac{1}{\mathbf{y}^* I_d \mathbf{x}}.$$

- The criterion in step 7 becomes

$$\|A\mathbf{x} - s_{k+1} I_d \mathbf{x}\|_2 < \epsilon.$$

- Algorithm 2:

- Replace  $I$  by  $I_d$  in step 4 and 5.
- Replace step 6 and 7 by

$$\begin{aligned} X &= \text{Expand}(X, R, I_d \cdot L, \mathbf{x}), \\ Y &= \text{Expand}(Y, L, I_d \cdot R, \mathbf{y}). \end{aligned}$$

- In step 8, use  $G = Y^* I_d X$ .
- The criterion in step 15 becomes

$$\|A\hat{\mathbf{x}}_1 - \hat{\lambda}_1 I_d \hat{\mathbf{x}}_1\|_2 < \epsilon.$$

- Algorithm 5:

- Replace step 16 and 17 by

$$\begin{aligned} \tilde{X} &= \text{Expand}(\tilde{X}, R, I_d \cdot L, X_j), \\ \tilde{Y} &= \text{Expand}(\tilde{Y}, L, I_d \cdot R, Y_j). \end{aligned}$$

All the experiments described in this paper were done using implementations that operate on the sparse descriptor system model.



## 4.2 Computational optimizations

If a large number of dominant poles is wanted, the search spaces  $X$  and  $Y$  may become very large. By imposing a certain maximum dimension  $k_{\max}$  for the search spaces, this can be controlled: when the dimension of  $X$  and  $Y$  reaches  $k_{\max}$ , they are reduced to dimension  $k_{\min} < k_{\max}$  by keeping the  $k_{\min}$  most dominant approximate eigentriplets. The process is restarted with the reduced  $X$  and  $Y$ , a concept known as implicit restarting [6, 19]. This procedure is continued until all poles are found.

The systems in step 4 and 5 of Alg. 2 can be solved with the same  $LU$ -factorization of  $(s_k I_d - A)$ , by using  $L$  and  $U$  in step 4 and  $U^*$  and  $L^*$  in step 5. Because in practice the sparse Jacobian is used, computation of the  $LU$ -factorization is inexpensive.

In step 3 of Alg. 2, the eigentriplet  $(\mu_{\min}, \mathbf{u}, \mathbf{v})$  of  $H^{-1}(s)$  must be computed. This triplet can be computed with inverse iteration [19], or, by noting that this eigentriplet corresponds to the eigentriplet  $(\theta_{\max}, \mathbf{u}, \mathbf{v})$  of  $H(s)$ , with  $\mu_{\min} = \theta_{\max}^{-1}$ , with the power method [19] applied to  $H(s)$ . Note that there is no need to compute  $H(s)$  explicitly. However, if the number of states of the system is large, and the number of inputs/outputs of matrix  $H(s)$  is large as well, applying the power or inverse iteration methods at every iteration may be expensive. It may then be more efficient to only compute a new eigentriplet  $(\mu_{\min}, \mathbf{u}, \mathbf{v})$  after a dominant pole has been found, or once every restart.

As more eigentriplets have converged, approximations of new eigentriplets may become poorer due to rounding errors in the orthogonalization phase and the already converged eigentriplets. It is therefore advised to take a small tolerance  $\epsilon = 10^{-10}$ . Besides that, if the residual for the current approximation drops below a certain tolerance  $\epsilon_r > \epsilon$ , one or more iterations may be saved by using generalized Rayleigh quotient iteration [21] to let the residual drop below  $\epsilon$ . In practice, a tolerance  $\epsilon_r = 10^{-5}$  is safe enough to avoid convergence to less dominant poles.

The SAMDP requires a single initial shift, even if more than one dominant pole is wanted, because the selection strategy automatically provides a new shift once a pole has converged. On the other hand, if one has special knowledge of the transfer function, for instance the approximate location of dominant poles, this information can be used by providing additional shifts to SAMDP. These shifts can then be used to accelerate the process of finding dominant poles.

As is also described in [6], one can easily change the selection strategy to use any of the existing indices of modal dominance [10, 22]. For instance, a good strategy for selecting dominant poles is: select the pole  $\lambda_i$  with largest  $\|R_i\|_2/|\operatorname{Re}(\lambda_i)|$  for a complex estimate, and the largest  $\|R_i\|_2/|\lambda_i|$  for a real estimate. Also other strategies, such as to select the approximation closest to some target, are possible.

Finally, the procedure can be automated even further by providing the desired maximum error  $|\|H(s)\|_2 - \|H_k(s)\|_2|$  for a certain frequency range: the procedure continues computing new poles until the error bound is reached. Note that such an error bound requires that the transfer function of the complete model is known for a range of  $s \in \mathbb{C}$  (which is usually the case for sparse descriptor systems).

## 4.3 General MIMO transfer functions ( $m \neq p$ )

For a general non-square transfer function  $H(s) = C^T(sI - A)^{-1}B \in \mathbb{C}^{p \times m}$  ( $p \neq m$ ), the objective function (3) cannot be used, because the eigendecomposition is only defined for square matrices. However, the singular value decomposition is defined for non-square matrices and hence the objective function becomes

$$f : \mathbb{C} \longrightarrow \mathbb{R} : s \longmapsto \frac{1}{\sigma_{\max}(H(s))}. \quad (8)$$

Let  $(\sigma_{\max}(s), \mathbf{u}(s), \mathbf{v}(s))$  be a singular triplet of  $H(s)$ , ie.  $H(s)\mathbf{v}(s) = \sigma_{\max}(s)\mathbf{u}(s)$  and  $H^*(s)\mathbf{u}(s) = \sigma_{\max}(s)\mathbf{v}(s)$ . It follows that  $H^*(s)H(s)\mathbf{v}(s) = \sigma_{\max}^2(s)\mathbf{v}(s)$ , so the objective function (8) can also be written as

$$f : \mathbb{C} \longrightarrow \mathbb{R} : s \longmapsto \frac{1}{\lambda_{\max}(H^*(s)H(s))}, \quad (9)$$

with  $\lambda_{\max} = \sigma_{\max}^2$ . Because  $f(s)$  in (9) is a function from  $\mathbb{C} \rightarrow \mathbb{R}$ , the derivative  $df(s)/ds : \mathbb{C} \rightarrow \mathbb{R}$  is not injective. A complex scalar  $z = a + jb \in \mathbb{C}$  can be represented by  $[a, b]^T \in \mathbb{R}^2$ . The partial derivatives of the objective function (9) become

$$\begin{aligned}\frac{\partial f}{\partial a}(s) &= \frac{1}{\lambda_{\max}^2(s)} \sigma_{\max}(s) (\mathbf{y}^* I_d \mathbf{x} + \mathbf{x}^* I_d \mathbf{y}), \\ \frac{\partial f}{\partial b}(s) &= \frac{1}{\lambda_{\max}^2(s)} j \sigma_{\max}(s) (\mathbf{x}^* I_d \mathbf{y} - \mathbf{y}^* I_d \mathbf{x}),\end{aligned}$$

where

$$\mathbf{y} = (sI - A)^{-1} B \mathbf{v}, \quad \mathbf{x} = (sI - A)^{-*} C \mathbf{u}.$$

The derivative of (9) then becomes

$$\nabla f = 2 \frac{\sigma_{\max}}{\lambda_{\max}^2(s)} [\operatorname{Re}(\mathbf{y}^* I_d \mathbf{x}), \operatorname{Im}(\mathbf{y}^* I_d \mathbf{x})],$$

where  $\operatorname{Re}(a + jb) = a$  and  $\operatorname{Im}(a + jb) = b$ . The Newton scheme is

$$\begin{aligned}\begin{bmatrix} \operatorname{Re}(s^{k+1}) \\ \operatorname{Im}(s^{k+1}) \end{bmatrix} &= \begin{bmatrix} \operatorname{Re}(s^k) \\ \operatorname{Im}(s^k) \end{bmatrix} - (\nabla f(s^k))^\dagger f(s^k) \\ &= \begin{bmatrix} \operatorname{Re}(s^k) \\ \operatorname{Im}(s^k) \end{bmatrix} - [\operatorname{Re}(\mathbf{y}^* I_d \mathbf{x}), \operatorname{Im}(\mathbf{y}^* I_d \mathbf{x})]^\dagger \sigma_{\max},\end{aligned}$$

where  $A^\dagger = A^*(AA^*)^{-1}$  denotes the pseudo-inverse of a matrix  $A \in \mathbb{C}^{n \times m}$  with  $\operatorname{rank}(A) = n$  ( $n \leq m$ ) [13].

This Newton scheme can be proven to have superlinear convergence locally. Because the SAMDP uses subspace acceleration, which accelerates the search for new directions, and relies on Rayleigh quotient iteration for nearly converged eigentriplets, it is expected that performance for square and non-square systems will be equally good, as is also confirmed by experiments.

## 5 Numerical Results

The algorithm was tested on a number of systems, for a number of different input and output matrices  $B$  and  $C$ . Here the results for the Brazilian Interconnected Power System (BIPS) are shown. The BIPS data corresponds to a year 1999 planning model, having 2,370 buses, 3,401 lines, 123 synchronous machines plus field excitation and speed-governor controls, 46 power system stabilizers, 4 static var compensators, two TCSCs equipped with oscillation damping controllers, and one large HVDC link. Each generator and associated controls is the aggregate model of a whole power plant. The BIPS model is linearized about an operating point having a total load of 46,000 MW, with the North-Northeast generators exporting 1,000 MW to the South-Southeast Region, through the planned 500 kV, series compensated North-South intertie.

The state space realization of the BIPS model has 1,664 states and the sparse, unreduced Jacobian has dimension 13,251. The sparse jacobian structure and the full eigenvalue spectrum, for this 1,664-state BIPS model, are pictured in [7]. Like the experiments in [6, 7], the practical implementation operates on the sparse unreduced Jacobian of the system, instead of on the dense state matrix  $A$ .

In the experiments, the convergence tolerance used was  $\epsilon = 10^{-10}$ . The spaces  $X$  and  $V$  were limited to size 10 ( $k_{\min} = 2$ ,  $k_{\max} = 10$ ). New orientation vectors  $\mathbf{u}$  and  $\mathbf{v}$  (see step 3 in Alg. 2) were only computed at restarts and after a pole had converged. All experiments were carried out in Matlab 6.5 [23] on an Intel Centrino Pentium 1.5 GHz with 512 MB RAM.

To demonstrate the performance of SAMDP, it was applied to two square transfer functions and two non-square transfer functions of BIPS to compute a number of dominant poles (complex conjugate pairs are counted as one pole). Table 1 shows the statistics of SAMDP for the transfer functions. The eigenvalue spectrum of the  $8 \times 8$  MIMO modal equivalent, whose sigma plots are

Table 1: Results of SAMDP for the  $8 \times 8$ ,  $28 \times 28$ ,  $8 \times 6$ , and  $28 \times 25$  transfer functions of the Brazilian Interconnected Power System (BIPS). Shift  $s_1 = 0.1i$ .

Transfer function	#poles	#states	#LU	Time (s)
$8 \times 8$	160	234	1336	970
$8 \times 8$	200	291	1600	1260
$28 \times 28$	120	199	4354	2740
$28 \times 28$	180	286	4694	3610
$28 \times 28$	200	326	4982	3960
$8 \times 6$	160	227	1087	870
$28 \times 25$	200	321	5425	4560

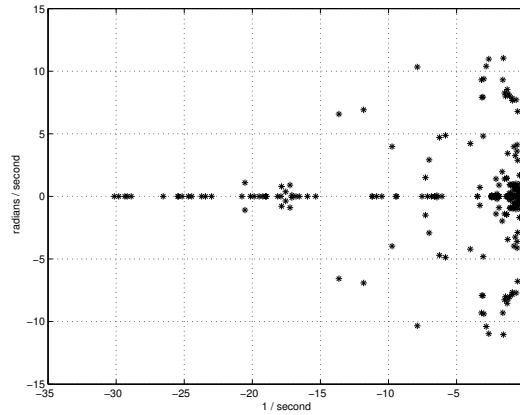


Figure 1: Pole spectrum of the 291st order modal equivalent of the  $8 \times 8$  transfer function.

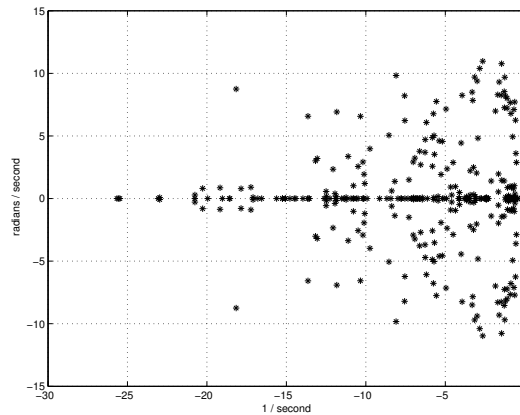


Figure 2: Pole spectrum of the 326th order modal equivalent of the  $28 \times 28$  transfer function.

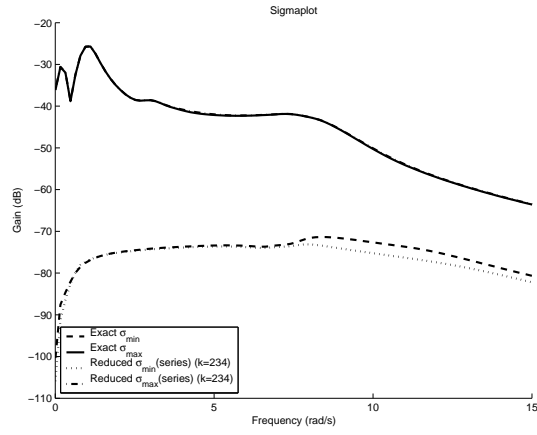


Figure 3: Sigma plot of modal equivalent and complete model for the  $8 \times 8$  Brazilian system transfer function (1,664 states in the complete model, 234 in the reduced model,  $\xi = 0\%$ ).

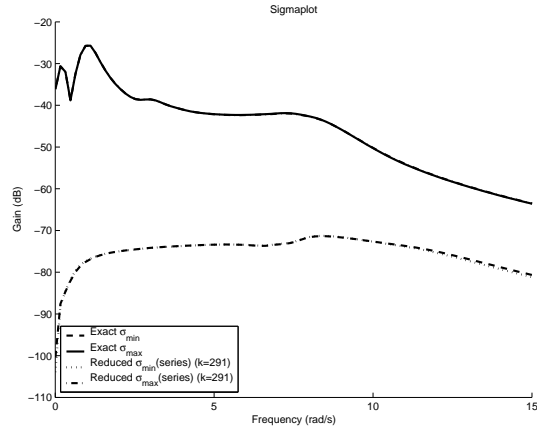


Figure 4: Sigma plot of modal equivalent and complete model for the  $8 \times 8$  Brazilian system transfer function (1,664 states in the complete model, 291 in the reduced model,  $\xi = 0\%$ ).

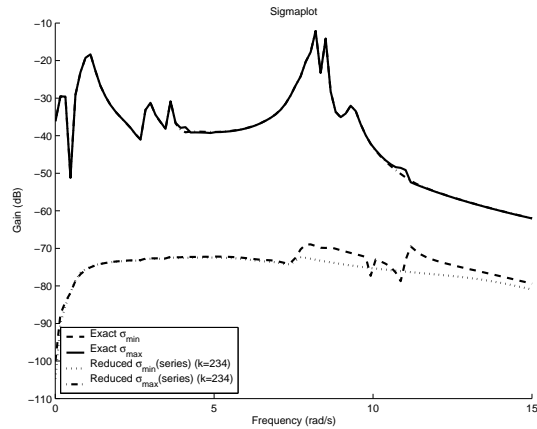


Figure 5: Sigma plot of modal equivalent and complete model for the  $8 \times 8$  Brazilian system transfer function (1,664 states in the complete model, 234 in the reduced model,  $\xi = 15\%$ ).

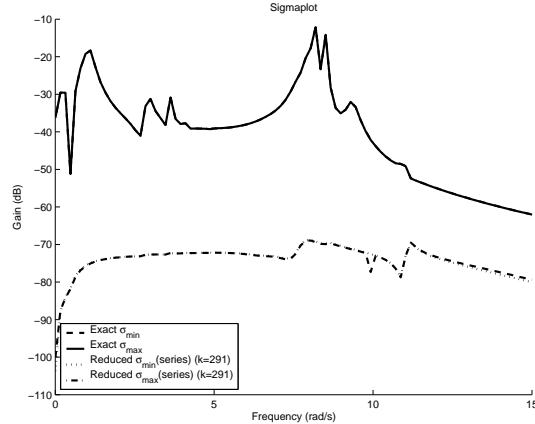


Figure 6: Sigma plot of modal equivalent and complete model for the  $8 \times 8$  Brazilian system transfer function (1,664 states in the complete model, 291 in the reduced model,  $\xi = 15\%$ ).

given in figures 4 and 6, is pictured in Fig. 1. The eigenvalue spectrum of the  $28 \times 28$  MIMO modal equivalent, whose sigma plot is given in Fig. 9, is pictured in Fig. 2.

SAMDP is able to automatically compute a modal equivalent for the  $8 \times 8$  transfer function of acceptable size that captures both the  $\sigma_{\min}$  and  $\sigma_{\max}$  curves very well, as shown in the sigma plots in figures 3 to 6. The  $8 \times 8$  transfer function is taken from [7], where a fairly low performance modal equivalent, having 39 states, was obtained through repeated MDP runs, in a procedure that required considerable human interaction. The reader is referred to [7] for more practical details on this  $8 \times 8$  power system transfer function and a complete list of the 39 dominant poles. Figures 5 and 6 shows sigma plots for a non-zero damping ratio  $\xi = 15\%$ . As is motivated in [7], sigma plots for non-zero damping ratios are helpful to identify dominant poles distant from the imaginary axis.

The second example is a  $28 \times 28$  transfer function of the BIPS model. Here one is in particular interested in a good fitting of the  $\sigma_{\max}$  curve: it will be used for estimating the major electromechanical modes, with applications in the damping analysis and control of power system oscillations. Matrix  $B \in \mathbb{R}^{n \times 28}$  is comprised of mechanical power input disturbance vectors for 28 generators, while  $C \in \mathbb{R}^{n \times 28}$  is comprised of output row vectors for the rotor speed deviations of the same generators. These 28 generators were selected for being of large size and also located in strategic parts of the BIPS, so that the MIMO function has good observability/controllability of the major system electromechanical modes. From figures 7 to 9 it can be observed that the SAMDP is able to approximate the  $\sigma_{\max}$ -curve well. Although not shown in the results, a good approximation of the  $\sigma_{\min}$  curve for this problem requires many more states in the modal equivalent.

Figures 10 and 11 show the  $\sigma_{\max}$  plots for the non-square  $8 \times 6$  and  $28 \times 25$  transfer functions, which were obtained by truncating the last columns of  $B$  of the  $8 \times 8$  and  $28 \times 28$  transfer functions respectively. The results confirm that SAMDP is also applicable to non-square transfer functions, with comparable performance.

It must be noted that all modal equivalents in this section are automatically computed by SAMDP, without human interaction, and can be reduced even further by neglecting less dominant contributions, or by application of the Balanced Model Reduction algorithm [10] to a state space realization of the modal equivalent, as described in a paper submitted to Trans. on Power Systems [24].

## 6 Conclusions

The SAMDP algorithm is a fast and robust method to compute dominant poles and corresponding residue matrices of both square and non-square MIMO transfer functions. The algorithm is

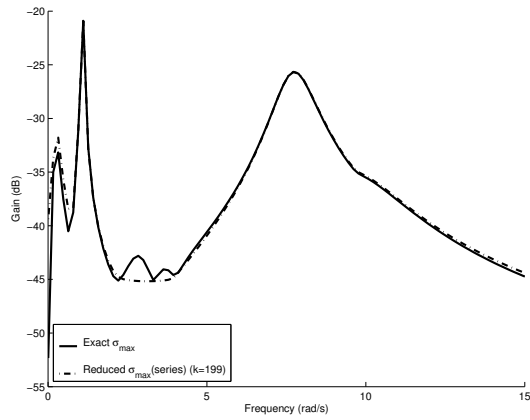


Figure 7: Sigma plot of modal equivalent and complete model for the  $28 \times 28$  Brazilian system transfer function (1,664 states in the complete model, 199 in the reduced model,  $\xi = 0\%$ ).

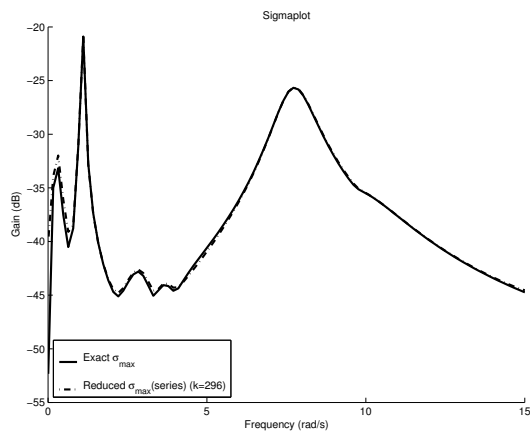


Figure 8: Sigma plot of modal equivalent and complete model for the  $28 \times 28$  Brazilian system transfer function (1,664 states in the complete model, 296 in the reduced model,  $\xi = 0\%$ ).

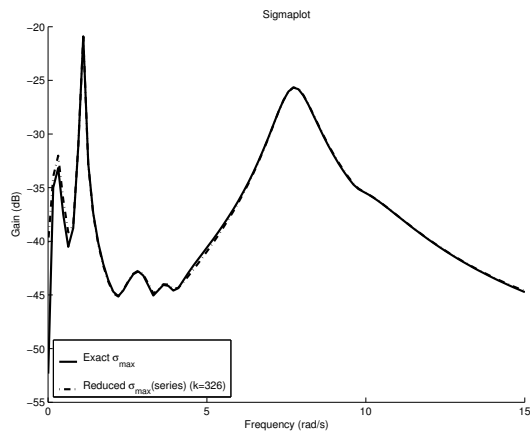


Figure 9: Sigma plot of modal equivalent and complete model for the  $28 \times 28$  Brazilian system transfer function (1,664 states in the complete model, 326 in the reduced model,  $\xi = 0\%$ ).

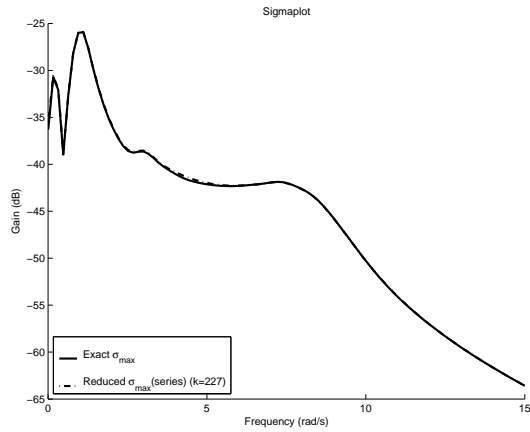


Figure 10: Sigma plot of modal equivalent and complete model for the  $8 \times 6$  Brazilian system transfer function (1,664 states in the complete model, 227 in the reduced model,  $\xi = 0\%$ ).

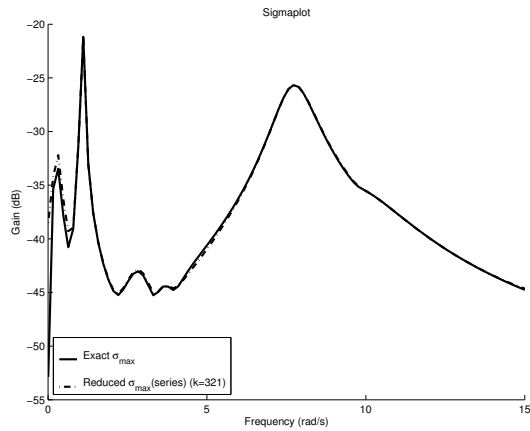


Figure 11: Sigma plot of modal equivalent and complete model for the  $28 \times 25$  Brazilian system transfer function (1,664 states in the complete model, 321 in the reduced model,  $\xi = 0\%$ ).

a variant of the SADPA [6] and has several advantages compared to existing methods: a natural selection method is used to converge to both real and complex dominant poles, subspace acceleration accelerates the algorithm and provides new pole estimates, and deflation techniques prevent the algorithm from (re-)computing already found poles. Finally, SAMDP is completely automatic: with a single shift, it is able to compute as many dominant poles as wanted, without intermediate human interaction.

The algorithm as presented in this article should be adequate for computer implementation by an experienced programmer. The paper results are related to the analysis and control of small signal stability, but the SAMDP algorithm is general and could be effectively applied to problems in other engineering fields that allow sparse descriptor system formulations. It can easily be adjusted to take advantage of specific properties or knowledge of the system.

## Acknowledgment

Both authors thank CEPEL and ELETROBRAS for providing the test systems.

## References

- [1] J. J. Sanchez-Gasca and J. H. Chow, "Power System Reduction to Simplify the Design of Damping Controllers for Interarea Oscillations," *IEEE Trans. Power Syst.*, vol. 11, no. 3, pp. 1342–1349, Aug 1996.
- [2] B. C. Pal, A. H. Coonick, and B. J. Cory, "Robust Damping of Inter-area Oscillations in Power Systems with Superconducting Magnetic Energy Storage Devices," *Proc. IEE Generation, Transmission and Distribution*, vol. 146, pp. 633–639, Nov 1999.
- [3] D. Chaniotis and M. A. Pai, "Model Reduction in Power Systems using Krylov Subspace Methods," *IEEE Trans. Power Syst.*, vol. 20, no. 2, pp. 888–894, May 2005.
- [4] A. Ramirez, A. Semlyen, and R. Iravani, "Order Reduction of the Dynamic Model of a Linear Weakly Periodic System-Part I: General Methodology," *IEEE Trans. Power Syst.*, vol. 19, no. 2, pp. 857–865, May 2004.
- [5] G. Troullinos, J. Dorsey, H. Wong, and J. Myers, "Reducing the Order of Very Large Power System Models," *IEEE Trans. Power Syst.*, vol. 3, no. 1, pp. 127–133, Feb 1988.
- [6] J. Rommes and N. Martins, "Efficient computation of transfer function dominant poles using subspace acceleration," Utrecht University, Preprint 1340, Dec. 2005, submitted to *IEEE Trans. Power Syst.*
- [7] N. Martins and P. E. M. Quintão, "Computing Dominant Poles of Power System Multivariable Transfer Functions," *IEEE Trans. Power Syst.*, vol. 18, no. 1, pp. 152–159, Feb 2003.
- [8] A. C. Antoulas and D. C. Sorensen, "Approximation of large-scale dynamical systems: an overview," *Int. J. Appl. Math. Comput. Sci.*, vol. 11, no. 5, pp. 1093–1121, 2001.
- [9] A. C. Antoulas, *Approximation of Large-Scale Dynamical Systems*. SIAM, 2005.
- [10] M. Green and D. J. N. Limebeer, *Linear Robust Control*. Prentice-Hall, 1995.
- [11] A. Varga, "Enhanced Modal Approach for Model Reduction," *Math. Mod. Syst.*, no. 1, pp. 91–105, 1995.
- [12] N. Martins, L. T. G. Lima, and H. J. C. P. Pinto, "Computing Dominant Poles of Power System Transfer Functions," *IEEE Trans. Power Syst.*, vol. 11, no. 1, pp. 162–170, Feb 1996.



- [13] G. H. Golub and C. F. van Loan, *Matrix Computations*, 3rd ed. John Hopkins University Press, 1996.
- [14] J. M. Maciejowski, *Multivariable Feedback Design*. Addison-Wesley, 1989.
- [15] T. Kailath, *Linear Systems*. Prentice-Hall, 1980.
- [16] J. R. Smith, J. F. Hauer, D. J. Trudnowski, F. Fatehi, and C. S. Woods, "Transfer Function Identification in Power System Application," *IEEE Trans. Power Syst.*, vol. 8, no. 3, pp. 1282–1290, Aug 1993.
- [17] R. V. Patel and N. Munro, *Multivariable System Theory and Design*. Pergamon, 1982.
- [18] D. V. Murthy and R. T. Haftka, "Derivatives of eigenvalues and eigenvectors of a general complex matrix," *Int. J. Num. Meth. Eng.*, vol. 26, pp. 293–311, 1988.
- [19] Y. Saad, *Numerical methods for large eigenvalue problems: theory and algorithms*. Manchester University Press, 1992.
- [20] B. N. Parlett, *The Symmetric Eigenvalue Problem*. Prentice Hall, 1980.
- [21] ———, "The Rayleigh Quotient Iteration and Some Generalizations for Nonnormal Matrices," *Math. Comp.*, vol. 28, no. 127, pp. 679–693, July 1974.
- [22] L. A. Aguirre, "Quantitative Measure of Modal Dominance for Continuous Systems," in *Proc. of the 32nd Conference on Decision and Control*, December 1993, pp. 2405–2410.
- [23] The Mathworks, Inc., "Matlab R13." [Online]. Available: <http://www.mathworks.com>
- [24] N. Martins, F. G. Silva, and P. C. Pellanda, "Utilizing Transfer Function Modal Equivalents of Low-order for the Design of Power Oscillation Damping Controllers in Large Power Systems," in *IEEE/PES General Meeting*, June 2005, pp. 2642–2648, enlarged version submitted to *IEEE Trans. Power Syst.*